Transactions of the **14th International Conference on Structural Mechanics in Reactor Technology** (SMiRT 14), Lyon, France, August 17-22, 1997 **J02/6**

Fast transient analysis of thin shell reinforced concrete structures with a Drucker-Prager model

Lopez Cela J.J.[(1)], **Casadei F.**[(2)], **Pegon P.**[(2)]
(1) Universidad de Castilla-La Mancha, Spain
(2) European Commission - Joint Research Centre - ISIS, Italy

ABSTRACT. A simple approach to the numerical modelling of thin shell reinforced concrete structures subjected to dynamic loads is presented. The bulk concrete material and the steel reinforcements are approximated by an assembly of homogeneous layers. A Drucker-Prager elasto-plastic law is used for the concrete and a visco-plastic regularization technique is applied in order to prevent appearance of unphysical strain localizations. The model offers good computational efficiency since it allows the use of shell elements instead of by far more expensive solid finite element representations. It is therefore quite effective at least in those cases where extreme phenomena such as relative slipping or detachment of the layers (which are not taken into account by this model) do not play a primary role.

INTRODUCTION

The scope of this work is to set up a simple but effective method for the numerical representation of thin reinforced concrete shell structures subjected to fast transient dynamic loadings such as impacts and explosions. The chosen approach is 'macroscopic', in that the structures to be studied are discretized by *shell* finite elements. A typical element is viewed as a sandwich composed of several layers, each one having its own, homogeneous material. For simplicity, no attempt is done to model relative motions of the layers due e.g. to slip or delamination phenomena. This of course reduces the applicability of the method to the cases (i.e., load regimes or parts of the time transients) where such extreme phenomena do not play a primary role.

The main advantages of the method are its simplicity and its high computational efficiency, due to the fact that a small number of relatively large shell elements are used to model a given structure in place of myriads of much smaller continuum elements. Another attractive property is that it is easily implemented as an extension in any general finite element computer code already containing (homogeneous) shell elements and a library of suitable materials. The formulation is such that any meaningful combination of layers and materials is easily obtained and the model can be used, with the limitations pointed out above, not only for the representation of reinforced concrete structures but also more generally for any composite material that admits a layered approximation.

The present model has been implemented in PLEXIS-3C, a general finite element computer code for fast transient analysis of 3-D fluid-structure systems [1]. The program has been jointly developed by the French Commissariat à l'Energie Atomique (CEA-CEN Saclay) and by the European Commission (EC-JRC Ispra). PLEXIS-3C offers a large library of finite elements, using both continuum and structural representations, and a series of material models including concrete and steel materials, and therefore allows for straightforward implementation of the layer-based technique described in this work. In addition, the code presents unique capabilities for the simulation of fluid-structure interactions. Both the structural and the fluid do-

mains can be represented within one single, fully coupled numerical analysis thanks to sophisticated, yet fully automatic, interfacing algorithms. These are capable of automatically detecting and properly treating even the geometrically most complex fluid-structure interfaces of the permanent type, see e.g. [2].

These features, combined with the present efficient representation of reinforced concrete shell-like structures, open the way to realistic numerical analyses of complex 3-D engineering applications, of which two demonstrative examples will be presented below. The first case is an impact on a natural-draught cooling tower, which is discretized by triangular layered shell elements. This 3-D problem is purely structural since the impact loading is simulated by an imposed external pressure. The second test case is an example of fully coupled fluid-structure analysis, a gas explosion in a reactor containment. The geometry is axisymmetric: the reactor's secondary containment and some of the main internal structures are modelled with layered conical shell elements, while continuum elements discretize the fluids (explosive bubble and air) contained within the reactor building.

MODELLING OF THIN SHELL REINFORCED CONCRETE STRUCTURES

The shell finite element formulations implemented in PLEXIS-3C have in common the basic assumption that *fibers* (straight lines across the thickness of the undeformed element) remain straight during deformation. This hypothesis is justified by the fact that, in order to be represented by shell elements, the structures must be relatively thin.

Fibers may or may not be initially normal to some element mid-plane, usually called the *reference surface*. If the orientation of the fibers with respect to the reference surface is allowed to change during deformation, then transverse shear strains and stresses are included in the model and one has a so-called Mindlin-Reissner formulation. Otherwise, no transverse shear effects are taken into account, and one has a Kirchhoff formulation.

For any of the shell theories adopted in PLEXIS-3C, the main step in the element formulation is the calculation of the internal nodal forces equivalent to the state of stress over the element, which are then used to solve the equilibrium equations. Use is made of the principle of virtual work which, at the element level, results in an expression of the type:

$$\underset{\sim}{F}^{\text{int}} = \int_{V^e} \underset{\sim}{B}^T \underset{\sim}{\sigma} dV \tag{1}$$

where $\underset{\sim}{F}^{\text{int}}$ is the vector of internal nodal forces for a given element e, V^e is the volume of the element *in the current configuration*, $\underset{\sim}{B}$ is the matrix of derivatives of the shape functions and $\underset{\sim}{\sigma}$ is the Cauchy stress tensor.

Because of the special nature of the shell thickness (z) direction, the previous integral is usually in the form (x and y being tangent to the reference surface):

$$\underset{\sim}{F}^{\text{int}} = \iint_{xy} \left(\int_z \underset{\sim}{B}^T \underset{\sim}{\sigma} dz \right) dx dy \tag{2}$$

and, because of the complexity of the functions involved (non-linearity of material behaviour, large strains, etc.) it is often best evaluated numerically:

$$\underset{\sim}{F}^{\text{int}} = \sum_{\xi=1}^{N_\xi} \sum_{\eta=1}^{N_\eta} W_\xi W_\eta \left[\sum_{\zeta=1}^{N_\zeta} (\underset{\sim}{B}^T \underset{\sim}{\sigma})_{\xi\eta\zeta} W_\zeta \right] \det J \tag{3}$$

The W coefficients are the weights of the numerical integration process (e.g., Gauss rule) and $\det J$ is the determinant of the Jacobian matrix that describes the transformation of the element volume into a normalized domain, characterized by the normalized coordinates ξ, η, ζ. In this way the function is evaluated only at a given number of sampling or integration points within the element.

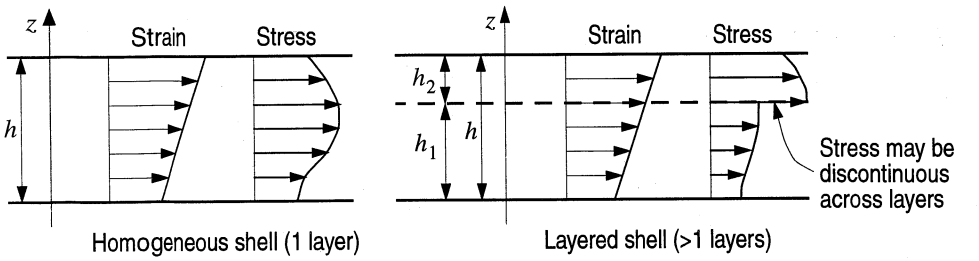

Figure 1 - Idealization of homogeneous and layered shell structures.

Let us now compare a homogeneous element with one composed by several layers, see Figure 1. In the homogeneous case, the stress profile across the thickness may assume complex shapes because of material non-linearities (e.g., plasticity), but is a continuous function. In the multilayer case, instead, if the materials of the various layers have different properties then the stress profile may become discontinuous across layers. The strain profiles are continuous in both cases because of the assumption of straight fibers. In order to compute the internal forces, we apply a procedure similar to (3), but now to each layer of the element separately:

$$\underset{\sim}{F}^{\text{int}} = \sum_{\xi=1}^{N_\xi} \sum_{\eta=1}^{N_\eta} W_\xi W_\eta \left\{ \sum_{L=1}^{N_L} \varphi_L \left[\sum_{\zeta_L=1}^{N_{\zeta_L}} (\underset{\sim}{B}^T \underset{\sim}{\sigma})_{\xi\eta\zeta_L} W_{\zeta_L} \right] \right\} \det J \qquad (4)$$

Here L is the layer index, which varies from 1 to N_L, the total number of layers. N_{ζ_L} is the number of Gauss integration points through the thickness in the layer L and ζ_L the normalized thickness coordinate for the layer. Finally, φ_L represents the ratio of the layer's thickness h_L to the total thickness h of the element: $\varphi_L = h_L/h$, hence $\sum_L \varphi_L = 1$.

APPLICATION EXAMPLES

As an example, consider the frequent case of concrete shell structures having reinforcement grids placed in two 'layers' within the bulk of concrete material, close to the inner and outer surfaces (this typical layout will be assumed in both numerical examples presented below.) If each grid has a large number of bars oriented along various directions, it can be approximated by an isotropic steel layer in the model. The layer thickness must be chosen so as to represent the real steel fraction present in the structure. The shell is then composed of 5 layers, of which 3 are of concrete and 2 of steel, see Figure 2. All layers have 1 integration point along the fiber, except the central one that, because of its thickness, has 2 Gauss points.

In Figure 2 a section across the thickness of a 2-D layered element is represented, where the concrete and steel layers as well as the location of the integration points are shown. For the presentation of results, all element quantities will be associated with a *lamina*, understanding

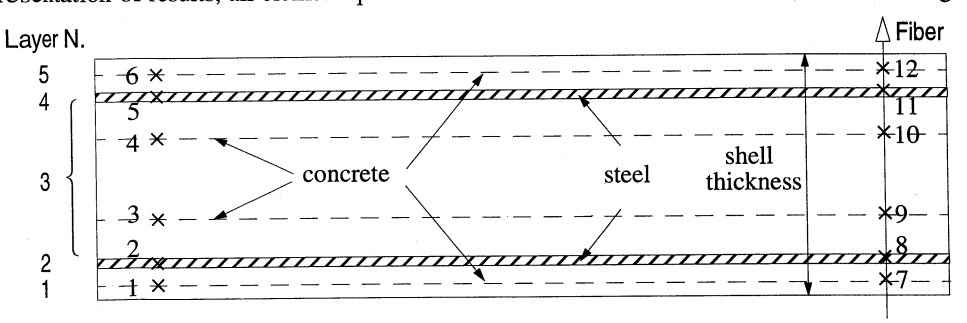

Figure 2 - Layered shell element: location of integration points along the thickness.

for that the plane containing all the integration points situated at the same height along a fiber. So, the example of Figure 2 is composed of 5 layers with 6 integration points altogether and consequently 6 laminae.

The steel is modelled with an elastic- perfectly plastic von Mises material while to represent the concrete the material model described in some detail in reference [3] is adopted: the well-known Drucker-Prager model (see e.g. [4]) is used for the inviscid, elasto-plastic behaviour of the concrete. The implementation, which uses the radial return algorithm, allows for hardening or softening and evolutions of the conical yield surface may occur either by displacement along the cone axis (constant *friction*) or by variation of the cone angle (constant *cohesion*). The algorithm includes a special treatment of the trial stress states that lie in the singular zone located near the apex of the conical yield surface.

One of the major numerical problems that affect the modelling of brittle materials is mesh dependency of solutions due to unphysical strain localizations either in the softening regime or, in the case of non-associative plasticity, even with positive hardening. Various regularization procedures have been proposed in order to avoid such effects, see e.g. [5]. One of these methods, which has been adopted here, is the introduction of visco-plastic terms in the material constitutive law, see also [6, 7] and [8].

The material properties for both examples are the following. For the steel, elastic- perfectly plastic behaviour with E = 210 GPa, ρ = 7800 kg/m^3, ν = 0.3, σ_{yield} = 680 MPa. For the concrete, elastoplastic behaviour with softening, E = 20 GPa, ρ = 2400 kg/m^3, ν = 0.2, dilatancy angle = 10°, maximum compression strength f_c = 40 MPa, maximum tension strength f_t = 4 MPa, and softening behaviour defined by the compression curve represented in Figure 3a. The viscoplastic parameter η defined in [3] will be determined separately in each example, because it depends not only on material parameters but also on the element's length.

Impact on a Cooling Tower

This example is concerned with a typical reinforced concrete structure, namely a natural-draught cooling tower. The main geometric, material and layer characteristics are shown in Figure 3a. Because of the symmetry, only one half of the structure has been modelled. The mesh is composed of 800 three-node triangular plate elements.

The criterion used to select the viscoplastic parameter η introduced (see [3]) in the material model in order to avoid localization problems, is $h/(\eta c) < 1$, where h is the characteristic element length of the mesh and c the sound speed in the material. One may obtain a good estimate of the ratio h/c by letting PLEXIS-3C (automatically) compute the critical time integration step $\Delta t = \min_e(h/c)$, where the minimum is taken over all elements in the mesh. The value is only approximated because the code uses a weighted average speed between those of concrete and of steel but, in any case, it is easier to proceed in this way than manually in a possibly quite complicated 3-D mesh. For this model, the code automatically computes Δt = 0.684 ms. Since PLEXIS-3C applies a safety factor of 0.5 the η parameter is:

$$\eta > \frac{\Delta t}{0.5} = 1.368\times10^{-3} \qquad \Rightarrow \qquad \eta = 2\times10^{-3} \tag{5}$$

The calculation was performed until a physical time of 100 ms. It required 148 time steps and 120 s of CPU on an HP 9000 712 workstation. In Figure 4 the equivalent plastic strain distributions are presented for the 4 concrete laminae at the final time. For ease of comparison, the same scale is used in all drawings. The strongest concentration of strain is located in lamina 6, that is the internal one. The pressure acts towards the centre of the tower, so the inner laminae 4 and 6 are under tension in the centre and therefore, the highest values of plastic strain are located in these zones.

Gas Explosion in a Reactor Containment

This example is a gas explosion within the reinforced concrete secondary containment building of a nuclear power plant. The geometry of the problem is given in Figure 3b and is assumed to be axisymmetric. The lower basement of the containment is vary thick and can be modelled by a rigid boundary. The building walls are relatively thin and can be conveniently represented by layered shell elements without a topological thickness. The containment is supposed to be initially filled by air at room temperature and atmospheric pressure. An explosion is assumed to take place in the lower part of the building at the initial time of the studied transient.

The explosive is simply represented by a perfect gas at high pressure, which initially occupies the zone indicated in black on Figure 5 ($t = 0$). The properties of this gas are: density $\rho = 111.5$ kg/m^3, adiabatic exponent $\gamma = 1.4$, specific internal energy $i = 1.28$ MJ/kg. The bulk air is also a perfect gas with $\rho = 1.2$ kg/m^3, $\gamma = 4$ and $i = 0.208$ MJ/kg. The characteristics of the structural materials are the same as for the previous example, and those corresponding to the layers are in the Table of Figure 3b. The mesh is composed of 981 continuum fluid elements (mostly 4-node quadrilaterals with a few 3-node triangles) and 88 conical shells. In this case, proceeding like in the previous example, one obtains $\Delta t = 0.0213$ ms, and therefore the viscosity parameter is:

$$\eta > \frac{\Delta t}{0.5} = 4.26\times10^{-5} \qquad \Rightarrow \qquad \eta = 7\times10^{-5} \tag{6}$$

The calculation required 11750 steps and 4120 s CPU on an HP 9000 712 workstation, for a physical time of 250 ms. Figure 5 shows the evolution of gas pressure within the containment in the first 120 ms; note the strong wave propagation and reflection effects. Figure 6 shows the deformations of the structures, amplified by a factor 10 to highlight the critical spots. The upper drawings correspond to the present case while the lower ones were obtained by assuming a purely elastic homogeneous material for the structures. Note that plasticity is reached in the present model's solution both at the containment top and, even more pronounced, at the inner horizontal floor, which appears to be seriously damaged at the end of the computed transient.

The examples have shown that the method is correctly implemented and may be applied to realistic analyses, with plausible results. However, a full validation and calibration campaign remains to be done, by comparison with experiments and other data available in the literature.

REFERENCES

1. Bung, H., Casadei, F., Halleux, J.P., Lepareux, M., 1989. *PLEXIS-3C: A Computer Code for Fast Dynamic Problems in Structures and Fluids.* SMiRT-10, Anaheim, 14-18 August.
2. Casadei, F., Halleux, J.P., 1995. *An Algorithm for Permanent Fluid-Structure Interaction in Explicit Transient Dynamics.* CMAME 128, pp. 231-289.
3. López Cela, J.J., Pegon, P., Casadei, F., 1997. *Fast Transient Analysis of Reinforced Concrete Structures with Drucker-Prager Model and Viscoplastic Regularization.* COMPLAS-5, Barcelona, Spain, March 17-20.
4. Loret, B., Prevost, J.H., 1986. *Accurate Numerical Solutions for Drucker-Prager Elastic-Plastic Models.* CMAME 54, pp. 59-277.
5. De Borst, R., Sluys, L.J., Mühlhaus, H.B., Pamin, J., 1993. *Fundamental Issues in Finite Element Analysis of Localization of Deformation.* Eng. Comp., 10, pp. 99-121.
6. Loret, B., Prevost, J.H., 1990. *Dynamic Strain Localization in Elasto-(Visco)Plastic Solids. Part 1. General Formulation and One-Dimensional Examples.* CMAME 83, pp. 247-273.
7. Prevost, J.H., Loret, B., 1990. *Dynamic Strain Localization in Elasto-(Visco)-Plastic Solids. Part 2. Plane Strain Examples.* CMAME 83, pp. 275-294.
8. Sluys, L.J. 1992. *Wave Propagation, Localisation and Dispersion in Softening Solids.* Ph D. Thesis, Technical University of Delft.

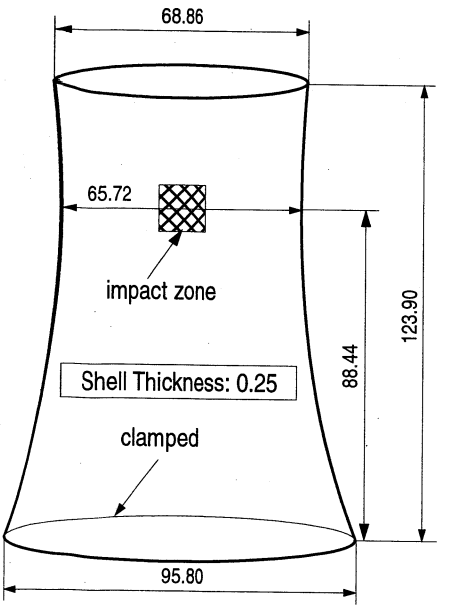

Layer N.	φ_L	Material
1	0.1	concrete
2	0.0025	steel
3	0.795	concrete
4	0.0025	steel
5	0.1	concrete

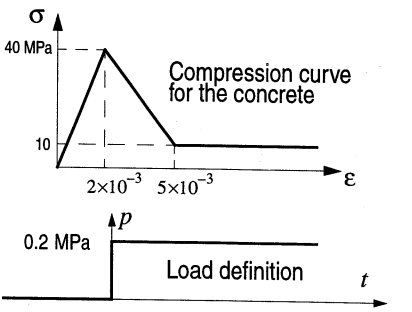

Figure 3 - a) Impact on a cooling tower: problem definition.

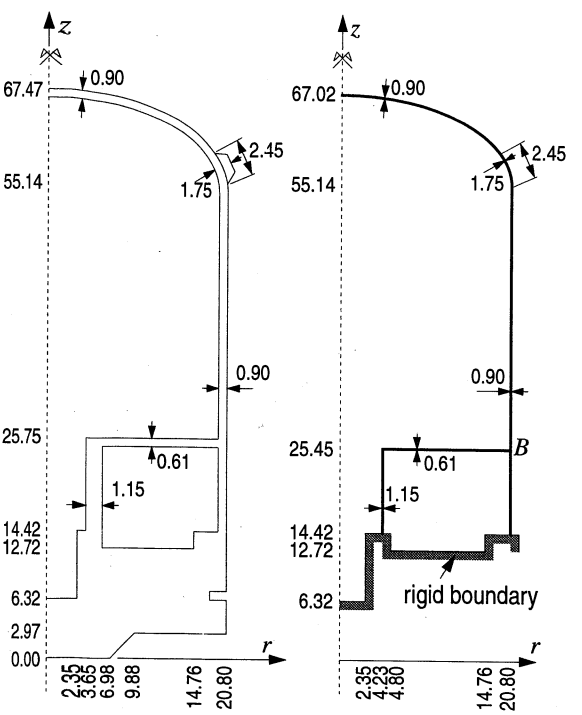

Layer N.	φ_L	Material
1	0.1	concrete
2	0.01	steel
3	0.78	concrete
4	0.01	steel
5	0.1	concrete

Figure 3 - b) Gas explosion in a reactor containment: problem definition.

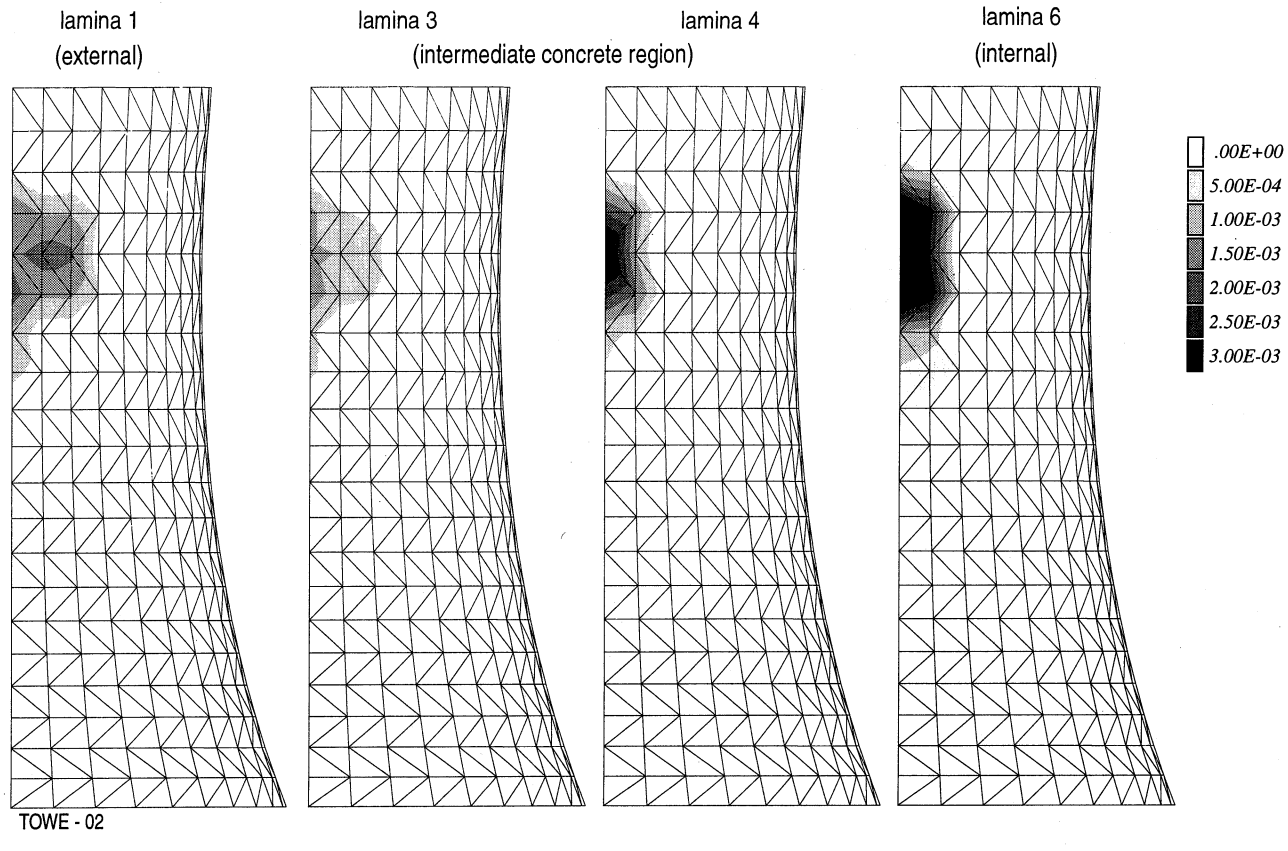

Figure 4 - Impact on a cooling tower: equivalent plastic strain distributions for the 4 concrete laminae at 100 ms.

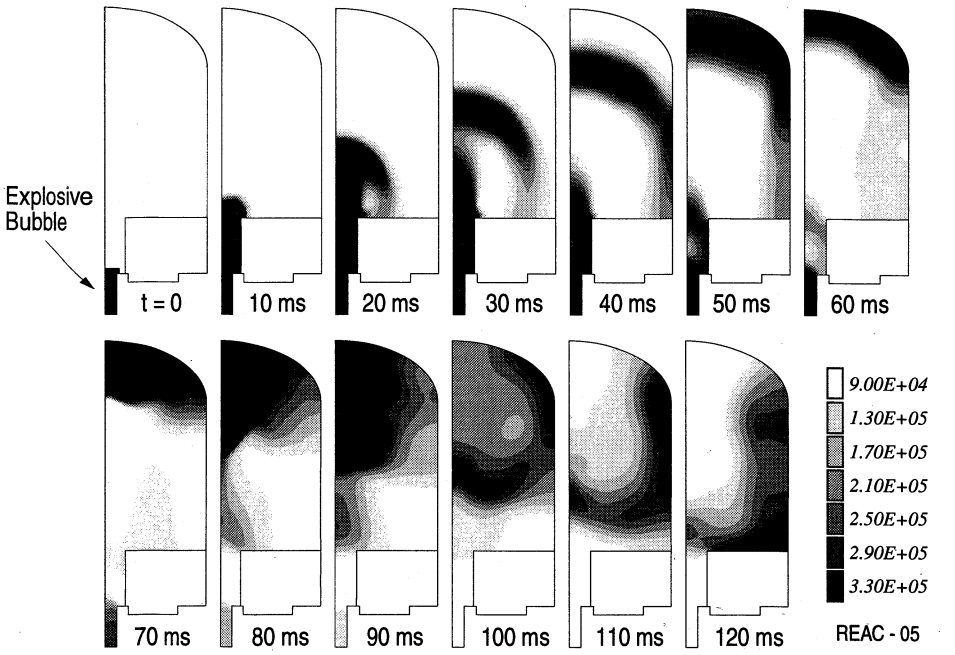

Figure 5 - Gas explosion in a reactor containment: fluid pressures.

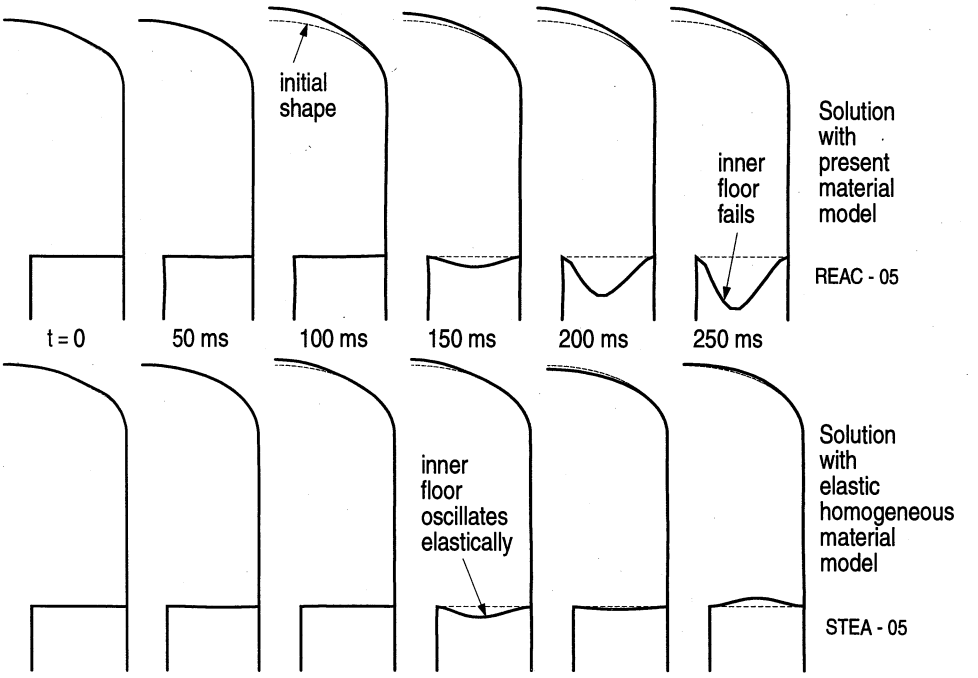

Figure 6 - Gas explosion in a reactor containment: structural deformations (x 10).